KEK-CP-211, UTHEP-561, YITP-08-46

S-parameter and pseudo-Nambu-Goldstone boson mass from lattice QCD

E. Shintani[a], S. Aoki[b,c], H. Fukaya[a,d], S. Hashimoto[a,e],
T. Kaneko[a,e], H. Matsufuru[a], T. Onogi[f], N. Yamada[a,e]
(JLQCD Collaboration)

[a] *High Energy Accelerator Research Organization (KEK), Tsukuba 305-0801,Japan*

[b] *Graduate School of Pure and Applied Sciences, University of Tsukuba, Tsukuba 305-8571, Japan*

[c] *Riken BNL Research Center, Brookhaven National Laboratory, Upton, New York 11973, USA*

[d] *The Niels Bohr Institute, The Niels Bohr International Academy, Blegdamsvej 17 DK-2100 Copenhagen Ø, Denmark*

[e] *School of High Energy Accelerator Science, The Graduate University for Advanced Studies (Sokendai), Tsukuba 305-0801, Japan*

[f] *Yukawa Institute for Theoretical Physics, Kyoto University, Kyoto 606-8502, Japan*

arXiv:0806.4222v2 [hep-lat] 3 Dec 2008

Abstract

We present a lattice calculation of L_{10}, one of the low energy constants in Chiral Perturbation Theory, and the charged-neutral pion squared mass splitting, using dynamical overlap fermion. Exact chiral symmetry of the overlap fermion allows us to reliably extract these quantities from the difference of the vacuum polarization functions for vector and axial-vector currents. In the context of the technicolor models, these two quantities are read as the S-parameter and the pseudo-Nambu-Goldstone boson mass respectively, and play an important role in discriminating the models from others. This calculation can serve as a feasibility study of the lattice techniques for more general technicolor gauge theories.

Spontaneous chiral symmetry breaking (SχSB) of strongly interacting gauge theory may provide a natural mechanism for the electroweak symmetry breaking. A class of new physics models based on this idea, so-called the technicolor models, has been studied extensively [1]. In most of those models, massless techni-quarks with weak charge are introduced; the weak gauge bosons acquire masses from their SχSB. The S-parameter may then be sizably affected, for which those models can be strongly constrained through the electroweak precision measurements [2]. Another characteristic signal of the technicolor models, that may be observed at the LHC experiments, is the presence of extra Nambu-Goldstone bosons (NGBs) which are not eaten by the weak gauge bosons. They are called the pseudo-NGBs (pNGBs), since they must be made massive by introducing explicit breaking of the chiral symmetry of the techni-quarks in a model dependent way, otherwise they would remain massless. Since the S-parameter and the pNGB mass are consequences of strong dynamics of the underlying theory, non-perturbative framework is required for their calculation. In previous studies, some model was involved in the calculation, *e.g.* [3].

In this work we consider two-flavor QCD as a testing ground of our method and demonstrate that the first principles calculation of those quantities are possible. In this context, the S-parameter corresponds to L_{10}^r (or l_5^r in another convention), one of the low-energy constants of the chiral perturbation theory (ChPT), as $S{=}-16\pi[L_{10}^r(\mu) - \{\ln(\mu^2/m_H^2) - 1/6\}/192\pi^2]$ with a renormalization scale μ and the Higgs mass m_H [2]. L_{10}^r is related to a difference of vacuum polarization functions between vector and axial-vector currents $\Pi_{V-A}^{(1)}(q^2) \equiv \Pi_V^{(1)}(q^2) - \Pi_A^{(1)}(q^2)$ near the zero momentum insertion. (A formula will be given in (5).)

For the pNGB mass, a mass formula that is valid for a wide range of technicolor models and breaking patterns is known [4]. The formula contains a nonperturbative part written in terms of the vacuum polarization functions. The charged pions in two-flavor QCD is an example of pNGB, as the electromagnetic interaction explicitly breaks $SU(2)$ chiral symmetry and gives a finite mass even in the massless limit of up and down quarks [5]. The corresponding mass formula is known as the Das-Guralnik-Mathur-Low-Young (DGMLY) sum rule [6]

$$m_{\pi^\pm}^2 = -\frac{3\alpha}{4\pi}\int_0^\infty dq^2\, \frac{q^2\, \Pi_{V-A}^{(1)}(q^2)|_{m_q=0}}{f^2}, \tag{1}$$

which gives the mass of charged pions at the leading order of the electromagnetic interaction. Here f denotes the pion decay constant in the chiral limit. Note that neutral pion is massless

in this limit.

In the continuum theory chiral symmetry guarantees that the difference $\Pi^{(1)}_{V-A}(q^2)$ exactly vanishes in the absence of both explicit and spontaneous chiral symmetry breaking. Any remaining difference in the absence of explicit breaking thus signals the SχSB. Therefore, the use of exactly chiral fermion formulation is mandatory in the lattice calculation, in order to avoid fake contributions to $\Pi^{(1)}_{V-A}(q^2)$ due to non-chiral lattice fermion formulations such as the Wilson-type fermions. Here we use the overlap fermion [7], which respects exact chiral symmetry at finite lattice spacings. Employing this fermion, we have successfully done a precise calculation of the chiral condensate [8], which also requires excellent chiral symmetry to control systematic errors.

We perform a two-flavor QCD calculation on a $16^3 \times 32$ lattice at a lattice spacing $a = 0.118(2)$ fm determined with the Sommer scale r_0=0.49 fm as an input [9]. The quark mass in the lattice unit is $\hat{m}_q = am_q =$ 0.015, 0.025, 0.035, and 0.050, which roughly cover the range between 1/6 to 1/2 of the strange quark mass. The global topological charge Q is fixed to ensure the exact chiral symmetry [9]. The main simulations are done in the Q=0 sector, using 10,000 trajectories. At $\hat{m}_q = 0.050$, the simulations are also performed in other two sectors ($Q = -2$ and -4) to estimate the finite volume effect due to fixing Q [10]. For each sea quark mass, the measurements are made at every 50 trajectories. Statistical errors are estimated from a jackknife analysis with 100 jackknife bins each containing two consecutive measurements. Details of our configuration generation and the pion spectrum and decay constant analysis are found in [9] and [11], respectively.

We calculate the current-current correlators for vector and axial-vector currents to obtain the corresponding vacuum polarization functions. We use as the vector current $V^{(12)}_\mu = Z\,\bar{q}_1\gamma_\mu(1 - aD/2m_0)q_2$, where q_1 and q_2 represent different flavors of quarks, D the overlap-Dirac operator in the massless limit, and m_0=1.6. The axial-vector current $A^{(12)}_\mu$ is the same but γ_μ is replaced by $\gamma_\mu\gamma_5$. The factor $(1-aD/2m_0)$ is necessary to make the V and A form an exact multiplet under the axial transformation. Because of this exact symmetry, then leading to the strong correlation, even the lattice artifacts and statistical fluctuations cancel between VV and AA correlators except for the effects of SχSB. Indeed, the statistical errors are much smaller than those of the previous calculations of the VV correlator [12]. The common renormalization constant $Z = 1.3842(3)$ is determined nonperturbatively [11].

Since the continuous rotational symmetry is violated on the lattice at $O(a^2)$ and the

currents we use are not conserved (cf. [13]), the general form of the current-current correlator reads

$$\begin{aligned}\Pi_{J\mu\nu}(\hat{q}) &= \sum_x e^{i\hat{q}\cdot x}\langle\, 0|\, T\left[J_\mu^{(21)}(x)J_\nu^{(12)}(0)\right]|0\,\rangle \\ &= \sum_{n=0}^{\infty} B_J^{(n)}(\hat{q}_\mu)^{2n}\delta_{\mu\nu} + \sum_{n,m=1}^{\infty} C_J^{(n,m)}(\hat{q}_\mu)^{2n-1}(\hat{q}_\nu)^{2m-1}, \end{aligned} \tag{2}$$

where $J = V$ or A. $B_J^{(n)}$ and $C_J^{(n,m)}$ are scalar functions of lattice momentum $\hat{q}_\mu{=}2\pi n_\mu/L$ with n_μ an integer ranging from $-L/2+1$ to $L/2$ (L=16 or 32 for spatial or temporal direction, respectively). In the continuum limit, only $B_J^{(0)}$ and $C_J^{(1,1)}$ survive. $B_J^{(0)}$ could contain a power divergent contribution due to a contact term, but the exact symmetry present between the vector and axial-vector currents guarantees that this contribution cancels in the difference $\Pi_{V\mu\nu} - \Pi_{A\mu\nu}$. Coefficients other than $B_J^{(0)}$ and $C_J^{(1,1)}$ represent lattice artifacts. In the difference $\Pi_{V\mu\nu} - \Pi_{A\mu\nu}$, these lattice artifacts are negligible as numerically confirmed below.

We define a measure of the Lorentz-violating lattice artifacts by

$$\Delta_J = \sum_{\mu,\nu} \hat{q}_\mu\hat{q}_\nu \left(\frac{1}{\hat{q}^2} - \frac{\hat{q}_\nu}{\sum_\lambda(\hat{q}_\lambda)^3}\right)\Pi_{J\mu\nu}, \tag{3}$$

which contains all of $B_J^{(n)}$ and $C_J^{(n,m)}$ but $B_J^{(0)}$ nor $C_J^{(1,1)}$. Figure 1 shows Δ_J for $J = V$ and A (top) and their difference (bottom) as a function of $\hat{q}^2$ at $\hat{m}_q$=0.015. While we observe statistically significant non-zero values of Δ_J depending on $\hat{q}^2$, the difference is orders of magnitude smaller than the individual Δ_J. Similar plot is obtained for $\hat{m}_q$=0.050. This indicates that the Lorentz-violating lattice artifacts indeed cancel in the difference $\Pi_{V\mu\nu} - \Pi_{A\mu\nu}$ and are insensitive to SχSB or m_q. Neglecting the Lorentz-violating terms, we analyze the difference

$$\Pi_{V\mu\nu} - \Pi_{A\mu\nu} = \left(\hat{q}^2\delta_{\mu\nu} - \hat{q}_\mu\hat{q}_\nu\right)\Pi_{V-A}^{(1)} - \hat{q}_\mu\hat{q}_\nu\Pi_{V-A}^{(0)}, \tag{4}$$

where $\Pi_{V-A}^{(1)}$ and $\Pi_{V-A}^{(0)}$ represent the transverse and longitudinal contributions, respectively.

First we calculate $L_{10}^r(\mu)$ from $\Pi_{V-A}^{(1)}$. At the next-to-leading order, ChPT predicts [14]

$$\Pi_{V-A}^{(1)}(q^2) = -\frac{f_\pi^2}{q^2} - 8\,L_{10}^r(\mu) - \frac{\ln\left(\frac{m_\pi^2}{\mu^2}\right) + \frac{1}{3} - H(x)}{24\pi^2}, \tag{5}$$

$$H(x) = (1+x)\left[\sqrt{1+x}\,\ln\left(\frac{\sqrt{1+x}-1}{\sqrt{1+x}+1}\right) + 2\right], \tag{6}$$

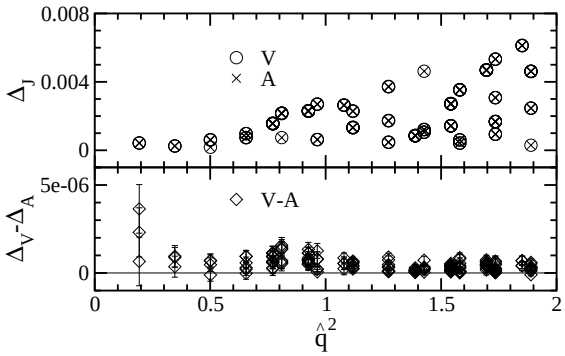

FIG. 1: $\hat{q}^2$ dependence of Δ_J ($J = V$ or A) (top) and their difference (bottom). The result for $\hat{m}_q$=0.015 is shown.

where $x \equiv 4m_\pi^2/q^2$, and μ is a renormalization scale set equal to the physical ρ meson mass m_ρ. Using the measured values of $\hat{m}_\pi$ and $\hat{f}_\pi$, we fit the data of $\hat{q}^2\Pi^{(1)}_{V-A}$ at four quark masses with (5) to obtain $L^r_{10}(m_\rho)$ varying fit range of $\hat{q}^2$. Correlation among the data points are ignored since each of all the data comes from different sea quark ensemble (also see below). It turns out that the fit including only the smallest $\hat{q}^2$ point ($\hat{q}^2$=0.038, which corresponds to (320 MeV)^2) gives an acceptable χ^2/dof (∼0.5). The fit is shown in Fig. 2 as a function of $\hat{m}_q$ (circles and solid curve). Once the second smallest $\hat{q}^2$ (∼ (650 MeV)^2 in the physical unit) is included the fit becomes unacceptable (χ^2/dof ∼ $O(40)$). This may indicate the breakdown of the chiral expansion at such a large q^2. Our result from the smallest $\hat{q}^2$ data is $L^r_{10}(m_\rho) = -5.22(17) \times 10^{-3}$. Here, the error is statistical only.

We estimate the systematic error due to higher order effects of the chiral expansion using a modified fit function to cover a wider range of $\hat{q}^2$ (see below). We obtain a slight negative shift, 0.3×10^{-3}, which is added to the systematic error. The finite size effect may be sizable in the pion-loop effects, which is the third term in (5), since the lattice volume (1.9 fm)^3 is not large enough. We estimate its magnitude by replacing the momentum integral with a sum. $\hat{f}_\pi$ and $\hat{m}_\pi$ are also corrected following [15]. Taking these corrections into account, we fit the data at the smallest $\hat{q}^2$ to (5) and obtain $L^r_{10}(m_\rho)|_{V=\infty} = -5.74(17) \times 10^{-3}$ with χ^2/dof= 2.3 as shown in Fig. 2 (triangles and dashed curve). We take the difference between these two results as an estimate of the systematic errors. We then quote

$$L^r_{10}(m_\rho) = -5.2(2)(^{+0}_{-3})(^{+5}_{-0}) \times 10^{-3}, \tag{7}$$

where the first error is statistical, and the second and third are the estimated systematic

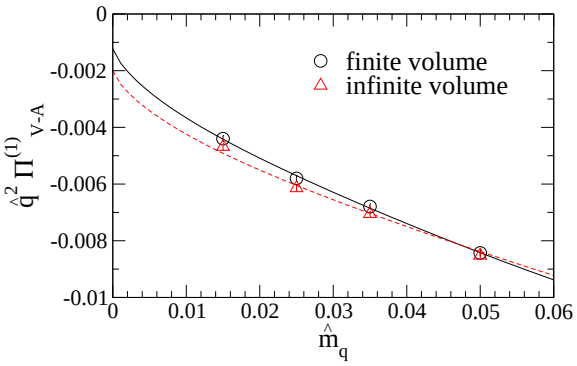

FIG. 2: $\hat{q}^2\Pi^{(1)}_{V-A}|_{\hat{q}^2=0.038}$ as a function of quark mass. The fit results with (solid) and without (dashed) finite volume correction are shown.

uncertainties due to higher order effects in q^2 and the finite size effect, respectively. Since only one value of $\hat{q}^2$ is included in the fit, the error from the chiral fit may be underestimated. Furthermore, other sources of uncertainty, *e.g.* finite lattice spacing and lack of a dynamical strange quark, exist. Nevertheless, (7) is already consistent with the experimental value $-5.09(47)\times 10^{-3}$ [16].

Next, we consider the squared-mass splitting between charged and neutral pions. The splitting in the chiral limit solely comes through the electromagnetic interaction and is written by the integral of $\hat{q}^2\Pi^{(1)}_{V-A}$ as given in (1). In order to avoid possibly large discretization effects in the large $\hat{q}^2$ region, we separate the whole integral region into two parts at $\hat{q}^2$=2.0, and estimate each part as follows.

For the lower $\hat{q}^2$ region (≤ 2.0), we fit the data to an ansatz

$$\hat{q}^2\Pi^{(1),\mathrm{fit}}_{V-A}(\hat{q}^2) \;=\; -\hat{f}_\pi^2 + \frac{\hat{q}^2\,\hat{f}_V^2}{\hat{q}^2+\hat{m}_V^2} - \frac{\hat{q}^2\,\hat{f}_A^2}{\hat{q}^2+\hat{m}_A^2} - \frac{\hat{q}^2}{24\pi^2}\,\frac{X(\hat{q}^2)}{1+x_5\,(Q_\rho^2)^4}, \tag{8}$$

where $Q_\rho^2 = \hat{q}^2/\hat{m}_\rho^2$ with $\hat{m}_\rho$ the physical ρ meson mass in lattice unit. Here and in the following x_i denotes a fit parameter. We introduce poles of the lowest-lying state for both vector and axial-vector channels with masses $\hat{m}_{V,A}$ and decay constants $\hat{f}_{V,A}$. We put the constraints $\hat{f}_\pi^2 = \hat{f}_V^2 - \hat{f}_A^2$ and $\hat{f}_A\hat{m}_A = \hat{f}_V\hat{m}_V$ among them so that they satisfy the first and second Weinberg sum rules [17]. We also assume a linear dependence on $\hat{m}_\pi^2$: $\hat{f}_V = x_1 + x_3\,\hat{m}_\pi^2$ and $\hat{m}_V = x_2 + x_4\,\hat{m}_\pi^2$. The function $X(\hat{q}^2)$ is either

$$\ln\left(\frac{\hat{m}_\pi^2}{\hat{m}_\rho^2}\right) + \frac{1}{3} - H(4\hat{m}_\pi^2/\hat{q}^2) + x_6\,Q_\rho^2, \tag{9}$$

$$\text{or} \quad x_6\,Q_\rho^2\ln(Q_\rho^2). \tag{10}$$

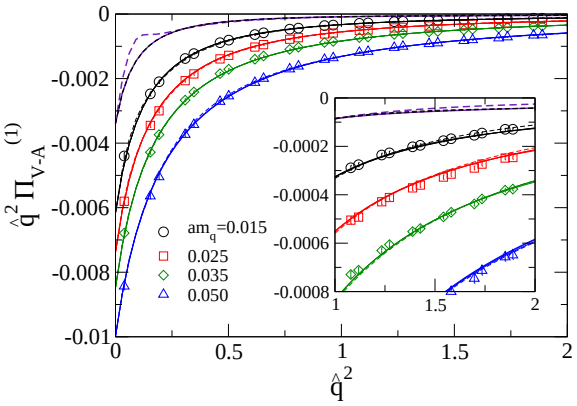

FIG. 3: The fit results with (9) (dashed curves) and (10) (solid curves). The results in the chiral limit are also shown. The statistical errors shown are smaller than the symbol size.

Then, the function (8) behaves as $O(q^{-6}, q^{-6}\ln q^2)$ at large q^2 in the chiral limit, which is consistent with the asymptotic scaling predicted by the operator product expansion (OPE) [18]. Taking (9) for $X(\hat{q}^2)$, $\Pi^{(1),\mathrm{fit}}_{V-A}(\hat{q}^2)$ reduces to the ChPT prediction (5) when $Q^2_\rho \ll 1$, while (10) gives a logarithmic term in the large Q^2_ρ region as expected by OPE.

We fit the data at $\hat{q}^2 \leq 2.0$ using the measured values of $\hat{f}_\pi$ and $\hat{m}_\pi$ as shown in Fig. 3. We have only attempted an uncorrelated fit since the full covariance matrix is likely ill-determined for many data points and free parameters in this fit. Both (9) and (10) fit the data quite well and indeed give a reasonable χ^2/dof, though the latter is slightly better. Integrating over $\hat{q}^2$ in the chiral limit, we obtain $m^2_{\pi\pm}|_{\hat{q}^2\leq 2.0}$= 676(50) and 811(12) MeV^2 for (9) and (10), respectively. The difference arises from the chiral extrapolation around $\hat{q}^2$=0.1–0.2, since (9) contains the chiral logarithmic term. Recalling that in the determination of L^r_{10} the ChPT formula fits the data only at the smallest $\hat{q}^2$ and (10) fits the data better than (9), we take the central value from the fit with (10) and the difference as a systematic error due to the chiral extrapolation.

Expanding $\hat{q}^2\Pi^{(1),\mathrm{fit}}_{V-A}$ around $\hat{q}^2 = 0$ in the chiral limit and comparing with (5), we obtain $L^r_{10}(m_\rho)= -\hat{f}^2\,(2x_1^2 - \hat{f}^2)/(8\,x_1^2x_2^2)$. With the fit results for (9), this gives $L^r_{10}(m_\rho) = -4.9\times 10^{-3}$. The difference from the central value is added to the systematic error from the higher order effect, and included in (7) as already mentioned.

The remaining part of the integral ($\hat{q}^2 \geq 2.0$) is estimated based on the OPE, which predicts $\Pi^{(1)}_{V-A}(q^2) \sim a_6/(q^2)^3$ in the chiral limit for large q^2 up to a logarithmic term. Assuming $\Pi^{(1)}_{V-A}|_{\hat{m}_q=0} = a_6/(\hat{q}^2)^3$ at $\hat{q}^2$=2, the fit result with (10) gives a_6=−0.0035. In the

estimate of the final result, we use a phenomenological value in the range $[-0.001, -0.01]$ GeV^6 [19] to be conservative. An integral then gives $m^2_{\pi^\pm}|_{q^2\geq 2.0}$= 182(149) MeV^2.

Summing up the two parts, we obtain

$$m^2_{\pi^\pm} = 993(12)(^{+}_{-135}{}^{0})(149)\ \text{MeV}^2, \tag{11}$$

as the pion squared-mass splitting in the chiral limit. The first error is statistical; the second and third ones are due to the chiral extrapolation and the uncertainty in a_6. The result is reasonably consistent with the experimental value at the physical quark mass [1261 MeV^2]. In addition to the errors quantified above, other sources of systematic errors may still remain. We do not expect, however, substantial systematic errors other than those estimated above, since the integral is dominated by the $\hat{q}^2 \sim 0$ region where the integrand $\hat{q}^2\Pi^{(1)}_{V-A}/\hat{f}^2$ in the chiral limit is strongly constrained by the first Weinberg sum rule $[\hat{q}^2\Pi^{(1)}_{V-A}]_{\hat{q}^2=0}/\hat{f}^2$=1.

In this letter, we have demonstrated that the S-parameter and the pNGB mass can be calculated using the lattice QCD technique. Since these quantities are generated solely through SχSB, the exact chiral symmetry on the lattice plays an essential role to prohibit contaminations from the explicit breaking. The method is general and the application to other vector-like gauge theories with arbitrary number of colors and flavors is straightforward. Thus with this method the lattice technique is able to directly investigate physical quantities relevant for the LHC phenomenology. In addition to these quantities, we can also calculate a_6 and the strong coupling constant using the data in the large q^2 region. The results will be reported in a subsequent paper.

We thank M. Golterman for useful comments. The work of HF is supported by Nishina Memorial Foundation. This work is supported in part by the Grant-in-Aid of the Japanese Ministry of Education (Nos. 17740171, 18034011, 18340075, 18740167, 19540286, 19740121, 19740160, 20025010, 20340047). Numerical simulations are performed on Hitachi SR11000 and IBM System Blue Gene Solution at High Energy Accelerator Research Organization (KEK) under a support of its Large Scale Simulation Program (No. 07-16).

---

[1] S. Weinberg, Phys. Rev. D **13**, 974 (1976); L. Susskind, Phys. Rev. D **20**, 2619 (1979); For a recent review, see, for example, C. T. Hill and E. H. Simmons, Phys. Rept. **381**, 235 (2003) [Erratum-ibid. **390**, 553 (2004)].

[2] M. E. Peskin and T. Takeuchi, Phys. Rev. Lett. **65**, 964 (1990); Phys. Rev. D **46**, 381 (1992).

[3] For recent works along this line using the Schwinger-Dyson and Bethe-Salpeter equations, see, M. Harada, M. Kurachi and K. Yamawaki, Phys. Rev. D **70**, 033009 (2004); Prog. Theor. Phys. **115**, 765 (2006).

[4] M. E. Peskin, Nucl. Phys. B **175**, 197 (1980): J. Preskill, Nucl. Phys. B **177**, 21 (1981).

[5] For the argument based on symmetry, see, for example, T. Blum *et al.* [RBC Collaboration], Phys. Rev. D **76**, 114508 (2007).

[6] T. Das *et al.*, Phys. Rev. Lett. **18**, 759 (1967).

[7] H. Neuberger, Phys. Lett. B **417**, 141 (1998); Phys. Lett. B **427**, 353 (1998).

[8] H. Fukaya *et al.* [JLQCD and TWQCD collaboration], Phys. Rev. Lett. **98**, 172001 (2007); Phys. Rev. D **76**, 054503 (2007); Phys. Rev. D **77**, 074503 (2008).

[9] S. Aoki *et al.* [JLQCD Collaboration], Phys. Rev. D **78**, 014508 (2008).

[10] S. Aoki *et al.*, Phys. Rev. D **76**, 054508 (2007).

[11] J. Noaki *et al.* [JLQCD Collaboration], PoS **LAT2007**, 126 (2007).

[12] T. Blum, Phys. Rev. Lett. **91**, 052001 (2003); M. Gockeler *et al.* [QCDSF Collaboration], Nucl. Phys. B **688**, 135 (2004); C. Aubin and T. Blum, Phys. Rev. D **75**, 114502 (2007).

[13] For the conseved currents, see Y. Kikukawa and A. Yamada, Nucl. Phys. B **547**, 413 (1999).

[14] J. Gasser and H. Leutwyler, Annals Phys. **158**, 142 (1984); Nucl. Phys. B **250**, 465 (1985).

[15] G. Colangelo, S. Durr and C. Haefeli, Nucl. Phys. B **721**, 136 (2005).

[16] G. Ecker, Acta Phys. Polon. B **38**, 2753 (2007).

[17] S. Weinberg, Phys. Rev. Lett. **18**, 507 (1967).

[18] See, for example, E. Braaten, S. Narison and A. Pich, Nucl. Phys. B **373**, 581 (1992).

[19] J. Bijnens, E. Gamiz and J. Prades, JHEP **0110**, 009 (2001); A. A. Almasy, K. Schilcher and H. Spiesberger, Eur. Phys. J. C **55**, 237 (2008).